Electrical Drives Control via Discrete-Time Variable Structure Systems

Invited paper

Čedomir Milosavljević
Faculty of Electrical Engineering, University of Istočno Sarajevo
Istočno Sarajevo, Bosnia and Hercegovina
cedomir.milosavljevic@elfak.ni.ac.rs

Branislava Peruničić Draženović, Senad Huseinbegović
Faculty of Electrical Engineering, University of Sarajevo
Sarajevo, Bosnia and Hercegovina

Boban Veselić, Milutin Petronijević
Faculty of Electronic Engineering, University of Niš
Niš, Serbia

Abstract— **Modern control techniques of electrical drives (EDs) use robust control algorithms. One of such algorithms is variable structure control (VSC) with sliding mode (SM). SM control needs more information on the controlled plant than the conventional PI(D) control. Valid mathematical model of the controlled plant is necessary for the SM controller design. Generalized mathematical model of two-phase electrical machine and its adaptation to direct current (DC) and induction motor (IM) are given in this paper, employed in the cascade control structure. Also, the basic SM control theory and discrete-time controller design approach, developed by the authors, are given. Finally, experimentally realized examples of speed and position control of DC and IM are given as an illustration of the efficiency of the promoted EDs controller design via discrete-time VSC.**

Keywords - electrical drives; sliding mode control; speed control; position control; discrete-time variable structure control;

I. INTRODUCTION

Electrical drives (EDs) are widely used in industry, transport, navigation, agriculture, home appliances, etc. Various types of electric motors are used in EDs. Direct current (DC) motors can be realized with parallel, series and combined excitation or can have permanent magnets (PM). Separately excited DC motors are a subclass of DC motors. They are preferably used in regulated drives, where especially constructed PM DC motors (servo motors) have dominant role. DC series motors are usually used in transportation because of their high starting torque. It can be fed by alternate current (AC) as well, known in that case as universal motor. The latter frequently used in home appliances. AC motors are induction motors (IMs) and synchronous motors (SMs). IMs can be single-phase, two-phase, three-phase or poly-phase. Their operation principle is based on Tesla's rotational magnetic field. IMs can have wounded rotor with rings and brushes at rotor shaft, when IM has two fed inputs, or with squirrel-cage rotor, when it has only one fed input. The latter is dominantly used in industry due to its robustness; it does not have rings nor brushes, does not produce sparks nor needs extra maintenance. It can be used in any conditions, even in water or explosive environment. Besides these types of motors, modern high quality controlled EDs can be realized with brushless DC motors or permanent magnet synchronous motors (PMSMs).

For regulation tasks with feedback control, DC servo motors have been initially used because of their excellent regulation characteristics: speed is a linear function of the applied armature voltage. On the other hand, their high price, demanding maintenance and inability to operate in every environment caused investigation and development of control methods for IMs. The breakthrough happened when Siemens engineer Blaschke [1] introduced the method of field-oriented control (FOC) or IM vector control. This progress became possible after advances in power electronics and microcomputers. By using FOC principle, IM as a multivariable and nonlinear dynamical element becomes similar to DC motor from the control aspect.

Mathematical model of the used motor, which has an important role in any modern control design of EDs, can be obtained from general motor model [2]. For this reason, we firstly introduce the generalized two-phase motor model in Section 2, from which the model of separately excited DC motor is derived in Section 3. Section 4 brings derivation of IM mathematical model and the main principle of FOC. The cascade control structure is presented in Section 5. Discrete-time (DT) sliding mode (SM) (DTSM) chattering-free controller design is given in Section 6, while Section 7 presents illustrative examples of practically realized DTSM controlled speed and positional servosystems with DC motors and IMs. Concluding remarks are given in Section 8.

II. GENERALIZED TWO-PHASE ELECTRICAL MACHINE MATHEMATICAL MODEL

In the control theory of EDs, the starting point is an idealized two-phase electrical machine whose mathematical model is the basis for any machine type. The ideal two-phase machine has two stator and two rotor windings. Axes of the stator (rotor) windings are perpendicular; therefore, there is no electromagnetic coupling between the stator (rotor) windings.

A. Lagrange equation-based model of electro-mechanical energy transformation

A dynamical model of a two-phase machine can be obtained by using the Lagrange equation [2],

$$\frac{d}{dt}\left\{\frac{\partial}{\partial\dot{\mathbf{q}}}L(\mathbf{q},\dot{\mathbf{q}})\right\}-\frac{\partial}{\partial\mathbf{q}}L(\mathbf{q},\dot{\mathbf{q}})+\frac{\partial}{\partial\dot{\mathbf{q}}}D(\mathbf{q},\dot{\mathbf{q}})=\mathbf{k}\,, \quad (2.1)$$

taking as generalized coordinates: the electrical charge in machine windings $\mathbf{q}_e$, the currents $\mathbf{i}$ flowing across windings (as analogies to angle and speed in mechanical systems) and the angle displacement and angular speed. Therefore, vectors of the generalized coordinates are:

$$\mathbf{q}=[\mathbf{q}_e \quad \theta_e]^{\mathrm{T}} \;;\; \dot{\mathbf{q}}=[\mathbf{i} \quad \omega_e]^{\mathrm{T}}. \quad (2.2)$$

$\mathbf{q}_e$ and $\mathbf{i}$ are vectors, but the electrical angular position θ_e and the electrical rotor speed ω_e are scalars; $\mathbf{k}$ is the total acting generalized force; $L(\mathbf{q},\dot{\mathbf{q}})$ is the Lagrange function representing the difference between kinetic and potential energy and D is the dissipative function.

Total kinetic energy arises from the electromagnetic energy in windings and the rotational mass of the rotor, i.e.

$$W_{k\,\Sigma}=W_{ke}+W_{km}=0.5(\mathbf{i}^{\mathrm{T}}\mathbf{L}\mathbf{i}+J\omega^2)\,. \quad (2.3)$$

where $\mathbf{L}$ is the matrix of inductances and J is the momentum of inertia.

Potential energy is zero since the torsion elasticity is assigned to the mechanical part of the electrical drive. Also, the electrical part of the motor does not contain capacitors.

The dissipative function is:

$$D(\mathbf{i},\omega)=0.5(\mathbf{i}^{\mathrm{T}}\mathbf{R}\mathbf{i}+B\omega^2)\,, \quad (2.4)$$

where $\mathbf{R}$ is the diagonal matrix $\mathbf{R}$=diag{$\mathbf{R}_s$,$\mathbf{R}_r$}; $\mathbf{R}_i$=diag{R_i}, i="s, r." Subscripts s and r denote, respectively, stator and rotor quantities. B is the coefficient of mechanical viscous friction.

The generalized force $\mathbf{k}$ that acts on the given system, is composed of the electrical potentials $\mathbf{u}$ and the load torque T_L, i.e.

$$\mathbf{k}=\begin{bmatrix}\mathbf{u} & -T_L\end{bmatrix}^{\mathrm{T}}. \quad (2.5)$$

Using (2.5) in (2.1), and taking into account that the Lagrange function is identical to the kinetic energy and does not depend on $\mathbf{q}_e$, equation (2.1) can be decomposed into the following equations:

$$\frac{d}{dt}(\mathbf{L}\mathbf{i})+\mathbf{R}\mathbf{i}=\mathbf{u}\,, \quad (2.6)$$

$$\frac{d}{dt}(J\omega)-\frac{1}{2}\frac{\partial}{\partial\theta_e}(\mathbf{i}^{\mathrm{T}}\mathbf{L}\mathbf{i})+B\omega=-T_L\,, \quad (2.7)$$

where $\mathbf{L}\mathbf{i}$ is the flux vector in (2.6). Eq. (2.7) contains mechanical quantities (inertia, friction and load torque). The second term on the left-hand side of (2.7) is the electromagnetic torque produced by the motor, i.e.

$$T_e=\frac{1}{2}\frac{\partial}{\partial\theta_e}(\mathbf{i}^{\mathrm{T}}\mathbf{L}\mathbf{i})\,. \quad (2.8)$$

Under the assumption that the stator (rotor) windings are identical and their axes are perpendicular, the matrices of resistances and inductances have the following forms:

$$\mathbf{R}=\begin{bmatrix}\mathbf{R}_s & \mathbf{0}\\ \mathbf{0} & \mathbf{R}_r\end{bmatrix},\ \mathbf{R}_s=R_s\mathbf{I},\ \mathbf{R}_r=R_r\mathbf{I};\ \mathbf{I}=\begin{bmatrix}1 & 0\\ 0 & 1\end{bmatrix}, \quad (2.9)$$

$$\begin{aligned}\mathbf{L}&=\begin{bmatrix}\mathbf{L}_s & \mathbf{L}_m\\ \mathbf{L}_m & \mathbf{L}_{\mathrm{r}}\end{bmatrix},\mathbf{L}_s=\begin{bmatrix}L_{\alpha\alpha} & L_{\alpha\beta}\\ L_{\beta\alpha} & L_{\beta\beta}\end{bmatrix}=L_s\mathbf{I};\\ \mathbf{L}_r&=\begin{bmatrix}L_{dd} & L_{dq}\\ L_{qd} & L_{qq}\end{bmatrix}=L_r\mathbf{I};\end{aligned} \quad (2.10)$$

$$\begin{aligned}\mathbf{L}_m&=\begin{bmatrix}L_{\alpha d} & L_{\alpha q}\\ L_{\beta d} & L_{\beta q}\end{bmatrix}=L_m\begin{bmatrix}\cos\theta_e & -\sin\theta_e\\ \sin\theta_e & \cos\theta_e\end{bmatrix}\\ &=L_m\mathbf{T}(\theta_e);\\ \mathbf{L}_m^{\mathrm{T}}&=L_m\mathbf{T}^{\mathrm{T}}(\theta_e).\end{aligned} \quad (2.11)$$

R_s, L_s (R_r, L_r) are, respectively, the resistance and inductance of the stator (rotor) windings. L_m is the mutual inductance between the stator and rotor windings when their magnetic axes are collinear. As can be seen, under the change of interposition of the stator and the rotor windings, the matrix of mutual inductances changes, and it is a function of rotor angle position and time since angle position changes with time.

Taking into account these propositions, (2.6) can be written in the form

$$\mathbf{L}\frac{d}{dt}\mathbf{i}+\frac{\partial\mathbf{L}}{\partial\theta_e}\frac{\partial\theta_e}{\partial t}\mathbf{i}+\mathbf{R}\mathbf{i}=\mathbf{u}\,, \quad (2.12)$$

where

$$\frac{\partial\theta_e}{\partial t}=\omega_e=p_p\omega\,. \quad (2.13)$$

p_p is the number of pole pairs of a two-phase machine and ω is the rotor mechanical speed. Eq. (2.12) becomes

$$\mathbf{L}\frac{d}{dt}\mathbf{i}+p_p\omega\frac{\partial\mathbf{L}}{\partial\theta_e}\mathbf{i}+\mathbf{R}\mathbf{i}=\mathbf{u}\,, \quad (2.14)$$

which, with (2.7) and (2.8), forms the generalized mathematical model of a two-phase electrical machine.

B. Park Coordinate transformation

Modern control techniques of IM (and PMSM as well) use the coordinate transformation of variables that participate in producing electromagnetic torque: currents, voltages and rotor and stator fluxes. These variables are related to one of the referent coordinate systems that are suitable for control. The principle of coordinate transformations is presented in Fig. 1. The stationary axes α,β are fixed to the stator windings axes; d,q axes are aligned to the rotor windings axes and rotate with the rotor speed, and u,v axes rotate with an arbitrary speed.

Consider the stator coordinate system α0β as the basic one. Then the rotor coordinate system $d0q$ is in position $\theta_e=\omega_e t$ while $u0v$ system is in position $\theta_k=\omega_k t$. Let a rotary vector $\mathbf{x}$ be in a certain position. Projections of this vector onto the stator and rotor coordinates are denoted as: x_α, x_β, x_d, x_q, respectively.

The task is to determine projections of the vector $\mathbf{x}$ on the coordinates u, v, using its projections onto coordinates α,β or d,q. According to Fig. 1, it is not difficult to obtain:

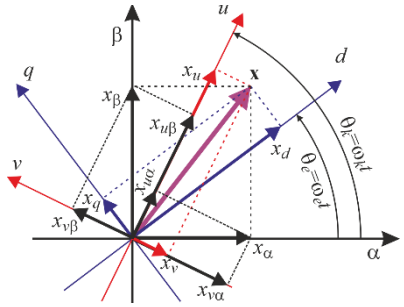

Figure 1. Coordinate transformations.

$$\begin{bmatrix}\mathbf{x}_u\\ \mathbf{x}_v\end{bmatrix}=\begin{bmatrix}\cos\theta_k & \sin\theta_k\\ -\sin\theta_k & \cos\theta_k\end{bmatrix}\begin{bmatrix}\mathbf{x}_\alpha\\ \mathbf{x}_\beta\end{bmatrix}=\mathbf{T}^{\mathrm{T}}(\theta_k)\begin{bmatrix}\mathbf{x}_\alpha\\ \mathbf{x}_\beta\end{bmatrix}, \quad (2.15)$$

$$\begin{bmatrix}\mathbf{x}_u\\ \mathbf{x}_v\end{bmatrix}=\begin{bmatrix}\cos(\theta_k-\theta_e) & \sin(\theta_k-\theta_e)\\ -\sin(\theta_k-\theta_e) & \cos(\theta_k-\theta_e)\end{bmatrix}\begin{bmatrix}\mathbf{x}_d\\ \mathbf{x}_q\end{bmatrix}=\mathbf{T}^{\mathrm{T}}(\theta_k-\theta_e)\begin{bmatrix}\mathbf{x}_d\\ \mathbf{x}_q\end{bmatrix}, \quad (2.16)$$

$$\begin{bmatrix}\mathbf{x}_d\\ \mathbf{x}_q\end{bmatrix}=\begin{bmatrix}\cos\theta_e & \sin\theta_e\\ -\sin\theta_e & \cos\theta_e\end{bmatrix}\begin{bmatrix}\mathbf{x}_\alpha\\ \mathbf{x}_\beta\end{bmatrix}=\mathbf{T}^{\mathrm{T}}(\theta_e)\begin{bmatrix}\mathbf{x}_\alpha\\ \mathbf{x}_\beta\end{bmatrix}. \quad (2.17)$$

Form of the transformation matrix **T** makes it's determinant equal to one, which gives:

$$\mathbf{T}^{-1}=\mathbf{T}^{\mathrm{T}};\quad \mathbf{T}\mathbf{T}^{\mathrm{T}}=\mathbf{T}^{\mathrm{T}}\mathbf{T}=\mathbf{I}. \quad (2.18)$$

I is the unity matrix. Besides, it is not difficult to obtain that

$$\mathbf{T}(\theta_e)\mathbf{T}^{\mathrm{T}}(\theta_k)=\mathbf{T}(\theta_k-\theta_e). \quad (2.19)$$

Now it is easy to write:

$$[x_\alpha\quad x_\beta]^{\mathrm{T}}=\mathbf{x}_{\alpha\beta}=[\mathbf{T}^{\mathrm{T}}(\theta_k)]^{-1}[x_u\quad x_v]^{\mathrm{T}}=\mathbf{T}(\theta_k)\mathbf{x}_{uv}=[\mathbf{T}^{\mathrm{T}}(\theta_e)]^{-1}[x_d\quad x_q]^{\mathrm{T}}=\mathbf{T}(\theta_e)\mathbf{x}_{dq}; \quad (2.20)$$

$$[x_d\quad x_q]^{\mathrm{T}}=\mathbf{x}_{dq}=[\mathbf{T}^{\mathrm{T}}(\theta_k-\theta_e)]^{-1}[x_u\quad x_v]^{\mathrm{T}}=\mathbf{T}(\theta_k-\theta_e)\mathbf{x}_{uv} \quad (2.21)$$

In the above relations, vector **x** may represent the vector of current, flux or voltage. By using (2.15) - (2.21) in (2.14) and (2.8), after not so complicated manipulations, the generalized mathematical model of two-phase motor is obtained as:

$$\begin{bmatrix}\mathbf{u}_{uvs}\\ \mathbf{u}_{uvr}\end{bmatrix}=\begin{bmatrix}\mathbf{R}_s & \mathbf{0}\\ \mathbf{0} & \mathbf{R}_r\end{bmatrix}\begin{bmatrix}\mathbf{i}_{uvs}\\ \mathbf{i}_{uvr}\end{bmatrix}+\begin{bmatrix}\omega_k\mathbf{J}\varphi_{uvs}\\ -\omega_{ke}\mathbf{J}\varphi_{uvr}\end{bmatrix}+\frac{\mathrm{d}}{\mathrm{d}t}\begin{bmatrix}\varphi_{uvs}\\ \varphi_{uvr}\end{bmatrix}, \quad (2.22)$$

where $\mathbf{J}=\begin{bmatrix}0 & 1\\ -1 & 0\end{bmatrix}$, $\omega_{ke}=\omega_k-\omega_e$.

Eq. (2.22) can be rewritten in the form

$$\begin{aligned}u_{us}&=R_s i_{us}+\frac{d}{dt}\varphi_{us}-\omega_k\varphi_{vs};\\ u_{vs}&=R_s i_{vs}+\frac{d}{dt}\varphi_{vs}+\omega_k\varphi_{us},\\ u_{ur}&=R_s i_{ur}+\frac{d}{dt}\varphi_{ur}-(\omega_k-\omega_e)\varphi_{vr};\\ u_{vr}&=R_s i_{vr}+\frac{d}{dt}\varphi_{vr}+(\omega_k-\omega_e)\varphi_{ur}.\end{aligned} \quad (2.23)$$

with additional equations for motor torque and fluxes:

$$T_e=\frac{p_p L_m}{L_s L_r-L_m^2}\left(\varphi_{ur}i_{vs}-\varphi_{us}i_{vr}\right); \quad (2.24)$$

$$\begin{aligned}\varphi_{us}&=L_s i_{us}+L_m i_{ur};\\ \varphi_{vs}&=L_s i_{vs}+L_m i_{vr};\\ \varphi_{ur}&=L_r i_{ur}+L_m i_{us};\\ \varphi_{vr}&=L_r i_{vr}+L_m i_{vs}.\end{aligned} \quad (2.25)$$

Model (2.23), (2.24) with (2.25) and (2.7) is the generalized model. It can be used for different reference coordinate systems: for the fixed stator frame (ω_k=0), for the rotor frame ω_k=ω_e or synchronously rotating frame of the electromagnetic field ω_k=ω_{0e}.

C. Clark two-phase to three-phase transformations

Since the three-phase IMs are the most frequently used in industry, and the two-phase machine model is the most suitable for its compactness, it is necessary to have a method for the transformation of a three-phase into the two-phase model and vice versa. To obtain these transformations, consider the three-phase and two-phase coordinate systems depicted in Fig. 2.

Vector **x** has projections onto coordinate axes of the three-phase (*abc*) and two-phase (αβ) coordinate systems. It is not difficult to obtain the following transformation equations:

$$\begin{bmatrix}x_a\\ x_b\\ x_c\end{bmatrix}=\begin{bmatrix}1 & 0\\ -0.5 & +0.5\sqrt{3}\\ -0.5 & -0.5\sqrt{3}\end{bmatrix}\begin{bmatrix}x_\alpha\\ x_\beta\end{bmatrix}, \quad (2.26)$$

$$\begin{bmatrix}x_\alpha\\ x_\beta\end{bmatrix}=\begin{bmatrix}1 & -0.5 & -0.5\\ 0 & 0.5\sqrt{3} & 0.5\sqrt{3}\end{bmatrix}\begin{bmatrix}x_a\\ x_b\\ x_c\end{bmatrix}. \quad (2.27)$$

Under the requirement that the transformation must preserve power (power must stay unchanged), it is necessary to introduce a correction factor of 3/2. This means that the three-phase motor torque is 3/2 times greater than one obtained by its two-phase model.

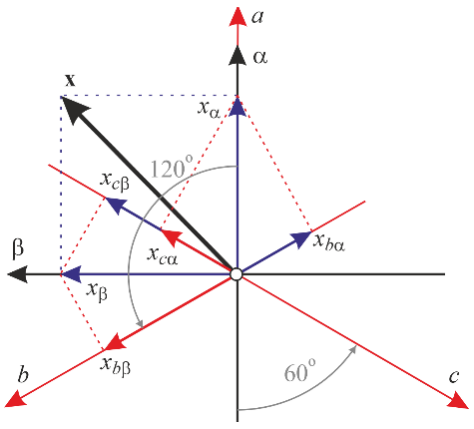

Figure 2. Two-phase to three-phase transformations.

III. DC MOTOR MATHEMATICAL MODEL

In DC motor, stator windings generate a stationary electromagnetic field. It is known from the electrical machine theory that for a motion, it is necessary that alternate current must flow in one of the motor windings. Therefore, DC motor rotor current changes as [2]:

$$\begin{aligned} &i_d = i_r \cos\theta_e; \quad i_q = -i_r \sin\theta_e \\ &i_{d\alpha} = i_r(\cos^2\theta_e + \sin^2\theta_e) = i_r \\ &i_{d\beta} = i_r(\cos\theta_e \sin\theta_e - \sin\theta_e \cos\theta_e) = 0 \end{aligned}, \qquad (3.1)$$

by using a commutator on the rotor shaft and brushes, resulting in current commutation from DC to AC.

A dynamical model of a separately excited DC motor is obtained by replacing $u_\beta = u_s$, $i_\beta = i_s$, $u_\alpha = u_q = 0$, $u_d = u_r$ $i_\alpha = i_q = 0$, in (2.23), which yields

$$\begin{aligned} u_s &= R_s i_s + L_s \frac{d}{dt} i_s, \\ u_r &= R_r i_r + L_r \frac{d}{dt} i_r + \omega_e L_m i_s, \\ T_e &= p_p L_m i_s i_r = k_t i_r. \end{aligned} \qquad (3.2)$$

Since $\omega_e = p_p \omega$ and if constant current, i_s=*const*. feeds stator winding, model (3.2) of a DC motor becomes linear:

$$\begin{aligned} u_r &= R_r i_r + L_r \frac{d}{dt} i_r + k_e \omega, \\ T_e &= k_t i_r, \end{aligned} \qquad (3.3)$$

with k_e and k_t having identical values in the corresponding units.

Since mechanical load is applied (friction and external load), the complete mathematical model of ED with DC motor for control purposes is:

$$\begin{aligned} \frac{d}{dt} i_r &= -\frac{R_r}{L_r} i_r - \frac{k_e}{L_r} \omega + \frac{1}{L_r} u_r, \\ \frac{d}{dt} \omega &= \frac{k_t}{J} i_r - \frac{B}{J} \omega - \frac{1}{J} T_L. \end{aligned} \qquad (3.4)$$

The first equation of (3.4) is solved with respect to i_r, under the condition $di_r / dt = 0$, and then the result is replaced into the second equation. This yield

$$\frac{d}{dt} \omega = -(a_m + \frac{B}{J})\omega + b_m u_r - \frac{1}{J} T_L, \qquad (3.5)$$

where $a_m = \frac{k_t k_e}{J R_r}$; $b_m = \frac{k_t}{J R_r}$.

Eq. (3.5) gives the model in which the speed is the controlled (state) variable, the rotor voltage u_r is the control variable and the current control loop dynamic is neglected. If the shaft position needs to be controlled, an additional equation

$$\frac{d}{dt} \theta = \omega \qquad (3.6)$$

must be added to (3.5). Hence, the complete DC motor dynamics can be expressed by standard state-space model

$$\begin{bmatrix} \dot{\theta} \\ \dot{\omega} \end{bmatrix} = \begin{bmatrix} 0 & 1 \\ 0 & -(a_m + \frac{B}{J}) \end{bmatrix} \begin{bmatrix} \theta \\ \omega \end{bmatrix} + \begin{bmatrix} 0 \\ b_m \end{bmatrix} u_r + \begin{bmatrix} 0 \\ b_L \end{bmatrix} T_L, \qquad (3.7)$$

with $b_L = -1/J$.

In the classical cascade control, the most inner current control loop should be designed using the first equation of (3.4). Then, the speed control loop is designed using the second equation of (3.4), where the rotor current i_r is the control variable.

IV. INDUCTION MOTOR MATHEMATICAL MODEL

The three-phase squirrel-cage IM is described by the mathematical model of the seventh-order: three differential equations for the stator, three for the rotor and one for the mechanical part. To simplify this three-phase model, it is transformed into the two-phase model that becomes [3]:

$$\dot{\mathbf{x}} = \mathbf{A}\mathbf{x} + \mathbf{B}\mathbf{u}, \qquad (4.1)$$

with:

$$\mathbf{x} = [i_{ds}, i_{qs}, \varphi_{dr}, \varphi_{qr}]^{\mathrm{T}}, \ \mathbf{u} = [u_{ds}, u_{qs}]^{\mathrm{T}},$$

$$\mathbf{A} = \begin{bmatrix} -\frac{R_s + \frac{R_r L_m^2}{L_r^2}}{\sigma L_s} & \omega_e & \frac{R_r L_m}{\sigma L_s L_r^2} & \frac{\omega_r L_m}{\sigma L_s L_r} \\ -\omega_e & -\frac{R_s + \frac{R_r L_m^2}{L_r^2}}{\sigma L_s} & -\frac{\omega_r L_m}{\sigma L_s L_r} & \frac{R_r L_m}{\sigma L_s L_r^2} \\ \frac{R_r L_m}{L_r} & 0 & -\frac{R_r}{L_r} & \omega_e - \omega_r \\ 0 & \frac{R_r L_m}{L_r} & -(\omega_e - \omega_r) & -\frac{R_r}{L_r} \end{bmatrix}$$

$$\mathbf{B} = \frac{1}{\sigma L_s} \begin{bmatrix} \mathbf{I} \\ \mathbf{0} \end{bmatrix}; \ \sigma = 1 - L_m^2 / (L_s L_r),$$

$$\frac{d}{dt} \omega = -(B/J)\omega + (1/J) T_e - (1/J) T_L, \qquad (4.2)$$

$$T_e = (3/2)(P_{\mathrm{p}} L_{\mathrm{m}} / L_{\mathrm{r}})(i_{qs} \varphi_{dr} - i_{ds} \varphi_{qr}). \qquad (4.3)$$

If the angle position is the output variable, an additional equation (3.6) completes the mathematical model.

A. Field oriented control (FOC) principle [1], [3]

The FOC (or vector control) principle, usually implemented by rotor flux-oriented control, ensures decoupling of torque control and rotor flux control. The rotor flux is aligned with the *d*-axis,

$$\varphi_{dr} = \varphi_r, \ \varphi_{qr} = 0 \ \wedge \ \frac{d}{dt} \varphi_{qr} = 0. \qquad (4.4)$$

According to (4.4), differential equation related to φ_{qr} becomes an algebraic equation

$$\omega_s = \omega_e - \omega_r = \omega_e - p_p\omega_m = L_m i_{qs} / (T_r\varphi_r), \qquad (4.5)$$

and differential equation related to φ_{dr} simplifies to

$$T_r\dot{\varphi}_r + \varphi_r = L_m i_{ds}. \qquad (4.6)$$

These equations define slip frequency and rotor flux dynamics. $T_r = L_r / R_r$ is the rotor time constant. The rotor flux is generated only by the flux current component i_{ds}. Since the rotor flux should be constant, the *d*-axis current controller should ensure that i_{ds} keeps a desired constant value i_{ds}^*. In a steady state $i_{ds} = i_{ds}^*$, and the rotor flux can be calculated using (4.6) as

$$\varphi_r = L_m i_{ds}^*. \qquad (4.7)$$

Substituting (4.4) and (4.7) into (4.3), the electromagnetic torque becomes

$$T_e = k_t i_{qs},\ k_t = (3p_p / 2)(L_m^2 / L_r) i_{ds}^* \qquad (4.8)$$

As a result, the electromagnetic torque is linearly dependent on the torque current component i_{qs}, indicating that both rotor flux and electromagnetic torque can be controlled separately as in separately excited DC motor.

By virtue of (4.5), (4.6), (4.7), and (4.8), and under the assumption that the flux current controller ensures $i_{ds} = i_{ds}^*$, IM model (4.1) – (4.4) is reduced to a third-order perturbed system, which is given by [3]

$$\begin{aligned}
&\dot{\mathbf{x}}_f = (\mathbf{A}_f + \Delta\mathbf{A}_f)\mathbf{x}_f + \mathbf{b}_f u + \mathbf{t}_f T_l,\ y = \mathbf{g}_f \mathbf{x}_f,\\
&\mathbf{x}_f = [x_{f1} \quad x_{f2} \quad x_{f3}]^{\mathrm{T}} = [\theta_m \quad \omega_m \quad i_{qs}]^{\mathrm{T}},\\
&\mathbf{A}_f = \begin{bmatrix} 0 & 1 & 0 \\ 0 & \frac{-B}{J} & \frac{k_t}{J} \\ 0 & 0 & \frac{-1}{T_{el}} \end{bmatrix},\ \Delta\mathbf{A}_f = \begin{bmatrix} 0 & 0 & 0 \\ 0 & 0 & 0 \\ 0 & \frac{-2k_t L_r}{3\sigma L_m^2} & \frac{-R_r}{\sigma L_r} \end{bmatrix}\\
&u = u_{qs}\\
&\mathbf{b}_f = \begin{bmatrix} 0 & 0 & \frac{1}{\sigma L_s} \end{bmatrix}^{\mathrm{T}},\ \mathbf{t}_f = \begin{bmatrix} 0 & \frac{-1}{J} & 0 \end{bmatrix}^{\mathrm{T}},\\
&\mathbf{g}_f = \begin{bmatrix} 1 & 0 & 0 \end{bmatrix}
\end{aligned} \qquad (4.9)$$

where $T_{el} = \sigma L_s / R_s$ is the electrical time constant. Parameter perturbation $\Delta\mathbf{A}_f$, which is due to the absence of decoupling circuits, is matched [4], i.e., $\mathrm{rank}[\mathbf{b}_f \mid \Delta\mathbf{A}_f] = \mathrm{rank}[\mathbf{b}_f]$, whereas the external disturbances are not.

In most IM vector control applications, two current controllers along with decoupling circuits are used as a part of inner control loops in addition to the position/velocity controller. Usually, hysteresis or PI current controllers are applied, but there are publications where sliding mode (SM) current controllers are applied too. The resulting current dynamics are much faster than the dynamics of mechanical part.

Further model simplification can be made if the electrical time constant is neglected since it is usually much smaller than the mechanical one. Model (4.9) is then reduced to a second-order perturbed system in a controllable canonical form [3]

$$\dot{\mathbf{x}} = (\mathbf{A} + \Delta\mathbf{A})\mathbf{x} + (\mathbf{b} + \Delta\mathbf{b})u + \mathbf{t}T_l, \qquad (4.10)$$

with

$$\begin{aligned}
&\mathbf{x} = [x_1 \quad x_2]^{\mathrm{T}} = [\theta_m \quad \omega_m]^{\mathrm{T}},\\
&\mathbf{A} = \begin{bmatrix} 0 & 1 \\ 0 & \frac{-B}{J} \end{bmatrix},\ \Delta\mathbf{A} = \begin{bmatrix} 0 & 0 \\ 0 & \frac{-2k_t^2 L_s L_r^2}{3JL_m^2(R_s L_r + R_r L_s)} \end{bmatrix},\\
&u = u_{qs},\\
&\mathbf{b} = \begin{bmatrix} 0 \\ \frac{k_t}{JR_s} \end{bmatrix},\ \Delta\mathbf{b} = \begin{bmatrix} 0 & \frac{-k_t R_r L_s}{JR_s(R_s L_r + R_r L_s)} \end{bmatrix}^{\mathrm{T}},\\
&\mathbf{b} = \begin{bmatrix} 0 \\ \frac{k_t}{JR_s} \end{bmatrix},\ \Delta\mathbf{b} = \begin{bmatrix} 0 & \frac{-k_t R_r L_s}{JR_s(R_s L_r + R_r L_s)} \end{bmatrix}^{\mathrm{T}}.
\end{aligned}$$

In this approximated model, the matching conditions are fulfilled; $\mathrm{rank}[\mathbf{b} \mid \Delta\mathbf{A} \mid \Delta\mathbf{b} \mid \mathbf{t}] = \mathrm{rank}[\mathbf{b}]$ If torque current controller and decoupling circuits were introduced, the input vector and perturbations in (4.10) would be $\Delta\mathbf{A} = \mathbf{0}$ and $\Delta\mathbf{b} = \mathbf{0}$, where $\mathbf{b} = [0 \quad k_t / J]^{\mathrm{T}}$, which is equivalent to model (4.2), (4.4) and (4.8). Since matching conditions hold, (4.10), without loss of generality, can be represented as

$$\dot{\mathbf{x}} = \mathbf{A}\mathbf{x} + \mathbf{b}u + \mathbf{j}v, \qquad (4.11)$$

where $\mathbf{j}v(t)$ is the matched equivalent disturbance, i.e., $\mathrm{rank}[\mathbf{b} \mid \mathbf{j}] = \mathrm{rank}[\mathbf{b}]$.

From the above explanation, it may be concluded that the method of vector control enables the mathematical models of DC motor (3.7) and IM (4.10) to be identical from the control design aspect.

V. Cascade Control of EDs

In EDs control practice, a cascade control structure is usually used, Fig. 3. Motor with controlled power supply (converter or inverter) and sensors represent controlled plant which input is control voltage *u*. The plant outputs that should be controlled are: electromagnetic torque T_e (current *i*), angular speed ω and angle position θ. To control these variables, a general control system contains current controller C_1, speed controller C_2 and position controller C_3. Each of controllers should have output saturation in order to limit maximum permissible value of the corresponding controlled variable. Limitation in the current controller C_1 is inherently present since supply voltage is (or must be) limited. Limitation at outputs of the speed controller C_2 and position controller C_3 should be introduced by designer in order to limit, respectively, motor current and motor speed to prevent over-current of motor (power supply) and over-speed of driven mechanism. From design aspect, the loop of the lower hierarchical level should be designed first, i.e., controller C_1 is firstly designed for control of object W_3. Then C_2 should be

designed for control of an object that represents series of W_2 and the equivalent dynamics of the closed-loop C_1, W_3, etc.

The given structure is general, but in many publications dedicated to EDs control can be found the separate treatment of position (speed) control without speed (current) loop.

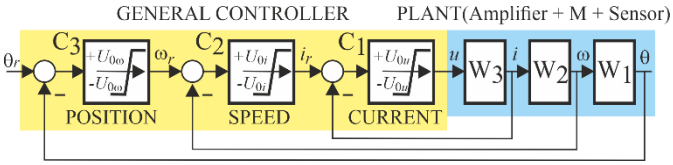

Figure 3. General cascade control structure of ED.

In the previous explanation, we indicate that DC and IM with FOC, from the controller design aspect, have the identical form of mathematical models. FOC control of IM is more complicated than DC motor control. A general cascade control structure for IM is given in Fig. 4, where the controlled plant in the broadest sense includes the following blocks: FOC scheme, controlled IM, power supply (inverter (VSI) with PWM), position and velocity sensors. Block of FOC scheme uses Park and Clark direct (inverse) transformation defined by matrix: $\mathbf{T}^{\mathrm{T}}(\theta_e)$ ($\mathbf{T}(\theta_e)$) and 3/2 (2/3).

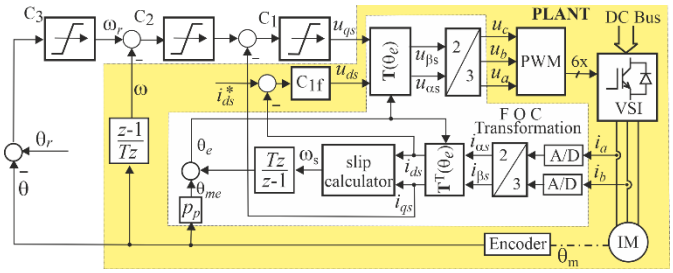

Figure 4. Block diagram of the IM position control.

Different techniques for controller design are used in the literature, starting from the conventional PI(D) controllers to the predictive controllers. This paper is intended to present the authors' experience in the control of EDs by using variable structure control systems with SM, employing DT signal processing. In the next section, after an introductory notation of SM essentials, some originally developed design methods will be presented, which are practically verified in control of EDs.

VI. DTSM Chattering-Free Control Algorithm

This section gives an introduction to SM control theory, then concisely describes an essential chattering-free DTSM control algorithm and a disturbance compensation method, and, finally, gives a modification of DT control algorithm for control of EDs.

A. *Introduction to SM*

Since dynamics of EDs for position (speed, torque (current)) control can be approximated by the second (first) order linear model, the following considerations are restricted only to this class of dynamical systems.

Consider the following continuous-time (CT) plant

$$\dot{\mathbf{x}}(t) = \mathbf{A}\mathbf{x}(t) + \mathbf{b}(u(t) + f(t)), \qquad (6.1)$$

where $\mathbf{x}(t) \in \Re^2$, $u(t)$, $f(t) \in \Re$ are, respectively, the state vector, the control and the bounded external disturbance $\left(\left|f(t)\right| \le f_0 < \infty, \forall t \ge 0\right)$. The pair (**A, b**) is assumed to be controllable, and the matrices **A, b** have appropriate dimensions. The matching conditions are satisfied since disturbance $f(t)$ acts through the control channel.

Let the model (6.1) be given in the controllable canonical form, i.e. $\dot{x}_1 = x_2$, as in (3.7), (4.10), where the state vector is

$$\mathbf{x} = [x_1 \; x_2]^{\mathrm{T}} = [\theta \;\; \omega]^{\mathrm{T}} \qquad (6.2)$$

Let the task be to control (6.1) in such a way that the system motion satisfies the relation

$$g(\mathbf{x}) = \mathbf{c}\mathbf{x} = 0, \; \mathbf{c} = [c \;\; 1], \; c > 0, \; \forall \mathbf{x}_0, t \ge t_1. \qquad (6.3)$$

Equation (6.3) in the state space $x_2 0 x_1$ represents a line

$$x_2 = -cx_1 \Leftrightarrow \dot{x}_1 = -cx_1. \qquad (6.4)$$

If the initial state is assumed to satisfy (6.3), then a stable motion $x_1 = x_0 e^{-ct}$ occurs, which does not depend on the plant parameters and control.

To obtain such motion for initial states not satisfying (6.3), control $u(t)$ should have two components: *reaching control* and *SM control.* The reaching control should bring the system state from any initial state and under any allowed disturbance to the line (6.3), while SM control should keep the system motion along that line afterward. The line $g(\mathbf{x})$=0 is denoted as *sliding line*, and function $g(\mathbf{x})$ is the *switching function (sliding variable).*

In SM control theory an additionally question arises: how to mathematically describe motion in SM, having in mind that the control that provides SM must be discontinuous.

Since in SM the system motion is kept on $g(\mathbf{x})$=0, then the condition $\dot{g}(\mathbf{x}) = 0$ must hold as well. Hence

$$\mathbf{c}\dot{\mathbf{x}}(t) = 0 \Rightarrow \mathbf{c}\mathbf{A}\mathbf{x}(t) + \mathbf{c}\mathbf{b}(u(t) + f(t)) = 0. \qquad (6.5)$$

Solving (6.5) with respect to control, under assumption **cb**=1, gives

$$u(t) = -\mathbf{c}\mathbf{A}\mathbf{x}(t) - f(t). \qquad (6.6)$$

In the nominal case, when $f(t)$=0 or, if it can be fully estimated and compensated, the control (6.6) becomes

$$u_{eq}(t) = -\mathbf{c}\mathbf{A}\mathbf{x}(t), \qquad (6.7)$$

which represents so-called *equivalent control.*

In the perturbed case (6.1), the control that establishes SM is given as

$$u(t) = u_{eq}(t) - \alpha \,\mathrm{sgn}(g), \;\; \alpha > 0, |f(t)| < \alpha. \qquad (6.8)$$

The second term control component in (6.8) $u_r(t) = -\alpha \,\mathrm{sgn}(g)$ is the reaching control and is the main cause of a parasitic motion excitation in the vicinity of the sliding line due to its discontinuous nature. These high-frequency oscillations are called *chattering*, which is an unwanted phenomenon in EDs control since it induces vibrations, mechanical wearing and performance degradation.

B. DT SM controller design [8], [14],[15],[19]

For DTSM design purposes, required by digital realization, model (6.1) has to be discretized. Usually, there are two methods: (*i*) to apply the traditional DT state-space model using zero-order hold (ZOH) and shift operator [5] or (*ii*) to use δ-state-space model [6]. In this paper, the δ- model is used for DT controller design since it is well suited for higher sampling frequencies [6], providing better accuracy of DSMC system [7], [8]. Fast sampling is of great interest in robotic applications for providing high-speed motion performance [9].

DT dynamical model of the nominal plant (6.1) ($f(t)$=0) in delta form is

$$\begin{aligned}\delta\mathbf{x}(kT) &= T^{-1}(x((k+1)T)-\mathbf{x}(kT)) \\ &= \mathbf{A}_\delta\mathbf{x}(kT)+\mathbf{b}_\delta u(kT)\end{aligned} \tag{6.9}$$

where T is the sampling period, $\mathbf{A}_\delta = T^{-1}(\mathbf{A}_d - \mathbf{I}); \mathbf{b}_\delta = T^{-1}\mathbf{b}_d$; k=0, 1, 2, ... Matrices $\mathbf{A}_d$ and $\mathbf{b}_d$ are from the traditional DT state-space shift model and may be obtained using single MATLAB command [Ad,bd]=c2d(A,b,T).

Remark 1. If (**A, b)** is a controllable pair, the pair ($\mathbf{A}_\delta$, $\mathbf{b}_\delta$) is also controllable for almost all choices of T.

Remark 2. For the sake of brevity, notation $\bullet_k$ stands for $\bullet(kT)$ in the rest of the paper.

Remark 3. In general, if matching conditions hold for (6.1) it does not necessarily follow that the same conditions hold for (6.9), because the ZOH does not exists in the disturbance channel. However, the corresponding error is $O(T^2)$ if a first-order disturbance compensator is used [13]. Therefore, it is reasonable to choose the sampling time T as small as possible.

Let the switching function that defines the sliding manifold be

$$g_k = \mathbf{c}_\delta\mathbf{x}_k, \mathbf{c}_\delta \in \Re^{1\times 2}. \tag{6.10}$$

Vector $\mathbf{c}_\delta$ defines the system behavior in DTSM. Its design will be given later. The switching function dynamics becomes

$$\delta g_k = T^{-1}(g_{k+1}-g_k) = \mathbf{c}_\delta\delta\mathbf{x}_k. \tag{6.11}$$

Solving (6.11) for g_{k+1} and replacing $\delta\mathbf{x}_k$ from (6.9) gives

$$g_{k+1} = g_k + T\mathbf{c}_\delta\mathbf{A}_\delta\mathbf{x}_k + T\mathbf{c}_\delta\mathbf{b}_\delta u_k. \tag{6.12}$$

The DTSM is defined with the following relation [7],[10]-[12]:

$$g_{k+1} = 0, \forall g(k). \tag{6.13}$$

Using (6.12) and (6.13), under the assumption $\mathbf{c}_\delta\mathbf{b}_\delta = 1$, the DTSM controls obtained as

$$u_{s,k} = -T^{-1}g_k - \mathbf{c}_\delta\mathbf{A}_\delta\mathbf{x}_k, \tag{6.14}$$

which contains two components. The first component $u_{r,k} = -T^{-1}g_k$ is the *reaching control*, which becomes zero after reaching the sliding manifold $g_k = 0$. The second component $u_{eq,k} = -\mathbf{c}_\delta\mathbf{A}_\delta\mathbf{x}_k$ becomes *equivalent control*, although (6.14) is at the same time the reaching and SM control. This property is not present in CTSM.

It is evident from (6.14) that for small T and $g_k \neq 0$ the control $u_{s,k}$ may be very high. Since in real systems control magnitude must be bounded, control (6.14) is modified as [8]

$$u_k = -c_\delta A_\delta x_k - \min\{\sigma, T^{-1}\,|\,g_k\,|\}\mathrm{sgn}(g_k) \tag{6.15a}$$

or [16]

$$u_k = U_0\,\mathrm{sat}\{[-\mathbf{c}_\delta\mathbf{A}_\delta\mathbf{x}_k - T^{-1}\,|\,g_k\,|\,\mathrm{sgn}(g_k)]\}. \tag{6.15b}$$

Note that $|\,g_k\,|\,\mathrm{sgn}(g_k) = g_k$. $\mathrm{sat}\{\bullet\} = \begin{cases}\mathrm{sgn}(\bullet) & \text{if } |\bullet|>1\\ \bullet & \text{if } |\bullet|\le 1\end{cases}$ takes into account the limitations of the control magnitude.

To finish the design, it is necessary to find a vector $\mathbf{c}_\delta$. The general comprehensive method [15] is used in this paper as a common approach for SM subspace design.

Under the assumption that $\mathbf{c}_\delta\mathbf{b}_\delta = 1$ it is obtained from [15]:

$$\mathbf{c}_\delta = [\mathrm{k}_\delta \;\; 1]\mathrm{pinv}[\mathbf{A}_\delta \;\; \mathbf{b}_\delta], \tag{6.16}$$

where

$$\mathbf{k}_\delta = \mathrm{place}(\mathbf{A}_\delta, \mathbf{b}_\delta, \Lambda_\delta) \tag{6.17}$$

is the gain vector of conventional state feedback, needed to provide the desired spectrum in δ-domain defined as

$$\Lambda_\delta = [\lambda_\delta, 0] \tag{6.18}$$

$$\lambda_\delta = T^{-1}(e^{\lambda T} - 1), \tag{6.19}$$

where λ, $\mathrm{Re}\{\lambda\} < 0$ is the desired eigenvalue in CT domain.

As shown in [8], the system (6.9) with the control (6.15) is robustly stable for bounded disturbances. Unfortunately, a steady-state error appears even if a constant type of disturbance is applied. To eliminate or lower the error, an additional integral action was proposed in [17] as a disturbance compensator, which is described in the next subsection

Remark 4. Another way to avoid a high initial control value is to apply integral DTSM (IDTSM). In this case, an integrator is added, whose initial condition is set to locate the system initial state at the sliding line.

IDTSMC is used for the control of first-order plants in this paper. The sliding function is then defined as

$$g_{k+1} = g_k + b_\delta(x_{k+1} - x_k) - T\lambda_\delta x_k, \tag{6.20}$$

where λ_δ is a real strongly stable eigenvalue.

Using the similar procedure, DTISM control becomes

$$\begin{aligned}u_k &= T^{-1}g_k + b_\delta^{-1}(a_\delta - \lambda_\delta)x_k \\ &= T^{-1}g_k + K_{eqI}x_k\end{aligned}. \tag{6.21}$$

C. Disturbance compensators synthesis [14], [19]

Now, consider the disturbed system (6.1), taking into account Remark 3. The DT model becomes

$$\delta\mathbf{x}_k = \mathbf{A}_\delta\mathbf{x}_k + \mathbf{b}_\delta(u_k + d_k), \tag{6.22}$$

$$d_k = \int_0^T e^{\mathbf{A}\tau}\mathbf{b}f((k+1)T-\tau))d\tau. \tag{6.22a}$$

The applied control is (6.14) and the assumption $\mathbf{c}_\delta \mathbf{b}_\delta = 1$ holds. Then, by replacing (6.14) in (6.22) and further in (6.11), $g(k+1)$ becomes

$$g_{k+1} = Td_k \text{ or } d_{k-1} = T^{-1} g_k . \tag{6.23}$$

Similar results have been obtained by Chan in [18], where a compensation algorithm was proposed.

To apply the approach [19], the value of the disturbance d_k should be reasonably well predicted from a finite number of its previous values, which is the case with typical disturbances in a real industrial environment. The control that theoretically cancels the disturbance in the system (6.22) is

$$u_{d,k} = u_k - d_k . \tag{6.24}$$

The procedure used to obtain (6.24) is the same as the one used to obtain (6.14). However, such control is not feasible since the present value of the disturbance is not known. Hence, the real disturbance term here is replaced by a compensational term denoted as $u_{c,k}$. Its role is to suppress the disturbance influence on the system state. Now, the total applied control is

$$u_{d,k} = u_k + u_{c,k} . \tag{6.25}$$

The switching function dynamics is then

$$\delta g_k = \mathbf{c}_\delta \mathbf{A}_\delta \mathbf{x}_k + (u_k + u_{c,k} + d_k). \tag{6.26}$$

Using (6.14), the future value of the switching function is

$$g_{k+1} = Tu_{c,k} + Td_k , \tag{6.27}$$

whereas the present value of the switching function becomes

$$g_k = Tu_{c,k-1} + Td_{k-1} . \tag{6.28}$$

Since the value of the switching function can be measured, and the value of the previous compensational control is known, it is possible to estimate the previous value of the disturbance as

$$d_{est,k-1} = T^{-1} g_k - u_{c,k-1} . \tag{6.29}$$

The subscript "*est*" in (6.29) denotes that estimated value may differ from the real one due to system parameter uncertainties. If the disturbance is slowly changing, (6.29) may be used as a reasonably good estimate of the present disturbance value.

The corresponding compensational control is

$$u_{c,k} = -d_{est,k-1} = -(T^{-1} g_k - u_{c,k-1}) . \tag{6.30}$$

To obtain a better dynamic, especially to prevent chattering in the system with unmodeled dynamics, it is not advisable to use full compensational control (6.30) but [17]

$$u_{c,k} = -(\alpha T^{-1} g_k - u_{c,k-1});\ 0 < \alpha \le 1 . \tag{6.30}$$

This is a recursive form of the compensational control, and its initial value has to be set. With this compensational control, the future value of the switching function will depend on the difference between the real and the estimated value of the disturbance

$$g_{k+1} = T(d_k - d_{est,k-1}) . \tag{6.31}$$

Obviously, the better disturbance estimation is used, the system behavior is closer to the nominal system.

The reasonable question would be how this additional compensational control affects the stability of the nominal system. First, consider the system with the theoretical equivalent control (6.24). The system has the disturbance d_k as an input, and the switching function g_k as an output. Application of *Z*-transform to equations (6.27) and (6.30), assuming zero initial conditions, gives

$$zg(z) = Tu_c(z) + Td(z)) . \tag{6.32}$$

$$u_c(z) = -\frac{\alpha}{T(1-z^{-1})} g(z) . \tag{6.33}$$

Replacing (6.33) into (6.31) and solving for $g(z)$ yields

$$g(z) = \frac{T(z-1)}{z(z-(1-\alpha))} d(z) . \tag{6.34}$$

It is obvious that $g(z)$ will be stable if $0 < \alpha \le 1$. This result was obtained in [17]. For $\alpha = 0$ the switching function dynamics is equivalent to the dynamics of the system without disturbance compensation ($g_k = Td_{k-1}$). For α=1 switching function dynamics may be identified as one step delayed difference of the disturbance scaled with factor *T*.

Remark 5. Similarly, the two previous samples of the disturbance (d_{k-2} and d_{k-1}) can be used for better estimation. In this case, the second-order disturbance compensator is obtained as [19]

$$u_{c2}(z) = \frac{(2z-1)z}{T(z-1)^2} \tag{6.35}$$

Remark 6. Another effective approach to estimate and compensate disturbances, named *active disturbance estimation* (ADE) [3], based on the model reference control method, is depicted in Fig. 5. In the ADE, the SMC controller may include the above DTSM controller with disturbance compensator (6.33). $G_n(z)$ is the nominal model of real process G(z), *d* is the disturbance and u_{in} is the output of the main controller.

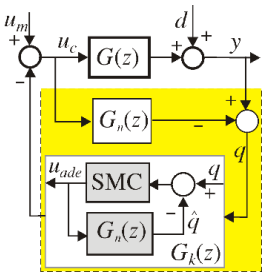

Figure 5. Active disturbance estimator.

D. Chattering problem

The SMC has a low sensitivity to parameter variations and disturbances, so it is attractive for high-performance servo systems. However, SMC quality depends on the possibility and validity of the obtained information about the state coordinates by using cheap sensors. That is the reason why state observers are used in many applications. The observers provide information about immeasurable states and can also reduce chattering [20]. In control practice, different types of observers are used: conventional Luenberger's observer of P-type or with additional integral action (PI or PI^2 observers [21]). There are also observers based on the SM principle. One of the more

popular in the last decade is the observer based on the second-order SM using the super-twisting algorithm [22]. For EDs control, particularly for IM FOC control, the position is usually detected by an incremental encoder. For the speed detection, an observer or differentiator should be used. Some authors used the third (second) order dynamical model for the position (speed) control of EDs. Then for the implementation of SM control, it is necessary to detect acceleration as well.

E. Modification of basic DTSM Control algorithm

The above control algorithms (6.15) could excite chattering in a real system. To suppress high chattering amplitude, two-scale reaching law can be used, which applies a smaller reaching control magnitude in a predefined vicinity of the sliding manifold [23].

Besides, the introduced integral action via disturbance compensator (6.33) causes undesirable overshoot. To eliminate the large overshoot, the compensator (6.33) needs also to be activated in a small vicinity of the sliding manifold. Therefore, as proposed in our previous work [26], a modification of the basic control algorithm, as well as disturbance compensator (6.34), gives a high-performance DTSM-based control system. The proposed control algorithm is described as

$$u_k = \begin{cases} U_0 \operatorname{sgn}(u_{\Sigma,k}), & u_{\Sigma,k} > \lvert U_0 \rvert \\ u_{\Sigma,k}, & u_{\Sigma,k} \le \lvert U_0 \rvert \end{cases} \tag{6.36a}$$

$$u_{\Sigma,k} = u_{eq,k} + u_{r,k} - u_{c,k} \tag{6.36b}$$

$$u_{r,k} = u_{r1,k} + u_{r2,k} \tag{6.36c}$$

$$u_{r1,k} = T^{-1} k_{r1} g_{\delta,k} \quad \text{if } u_{2,k} = \text{'0'} \tag{6.36d}$$

$$u_{r2,k} = T^{-1} k_{r2} g_{\delta,k} \quad \text{if } u_{2,k} = \text{'1'} \tag{6.36e}$$

$$0 < k_{r1,} k_{r2} < 1; \quad k_{r1} + k_{r2} \le 1 \tag{6.36f}$$

$$u_{2,k} = \begin{cases} \text{'0'}, & \lvert u_{\Sigma,k} \rvert > 0 \wedge u_{1,k-1} = \text{'0'} \\ \text{'1'}, & \lvert u_{\Sigma,k} \rvert \le 0 \wedge u_{1,k-1} = \text{'1'} \end{cases} \tag{6.36g}$$

$$u_{1,k} = \begin{cases} \text{'0'}, & \lvert u_{\Sigma,k} \rvert > 0 \\ \text{'1'}, & \lvert u_{\Sigma,k} \rvert \le 0 \end{cases} \tag{6.36h}$$

$$u_{c,k} = u_{c,k-1} + k_{int}^{\alpha} T \frac{g_{\delta,k}}{g_{\delta,k} + \beta} \tag{6.36i}$$

$$k_{int}^{\alpha} = k_{int}(1 + \gamma \lvert \operatorname{sat}(\delta r_k) \rvert) \tag{6.36j}$$

The block-structure presentation of (6.36) is given in Fig. 6.

VII. Realized EDs Control Via DTSM

This section illustrates some practically realized servo systems with DC motors and IMs, where speed and position control have been designed by the given approach.

A. Speed control of DC servo motors [14]

Since DC motor speed dynamics can be approximated by first-order dynamical equation (3.5), appropriate DTSM and DT integral SM controllers with combined disturbance compensator was proposed, as depicted in Fig. 7, for high-performance control. For details, see [14].

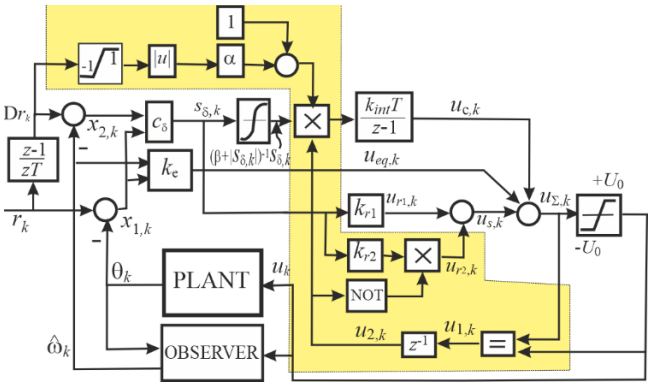

Figure 6. General control structure of a second-order plant via DTSM.

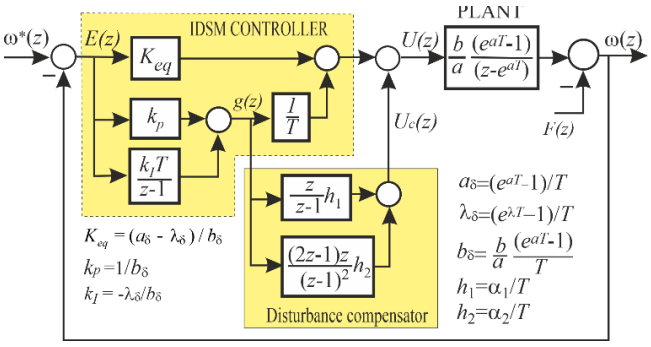

Figure 7. Block scheme of IDTSM velocity servo system in linear control mode. Disturbance compensator represents parallel connection of the first- (6.33) and the second-order (6.35) disturbance compensators.

The experimental platform, depicted in Fig. 8, uses a DC motor with the nominal parameters: $M_{\max} = 0.22$ Nm, $I_{\max} = 3.7$ A, $n_{\max} = 6000$ min^{-1}, $k_t = 0.056$ Nm/A, $k_e = 5.85$ V/1000 min^{-1}. A PWM power amplifier with the carrier frequency of 15 kHz drives the motor. A quadrature incremental encoder with 1000 lines is used for the position measurement. The plant parameters are identified as: $a_m = 26$, $b_m = 654$. Sampling time is T=1 ms. Parameters for the traditional DTSM(TDTSM) and integral DTSM (IDTSM) are given in Table I.

Some experimentally obtained results are presented in Figs. 9 and 10, clearly indicating that the proposed approach gives significant robustness improvement by applying disturbance compensator (6.33) in both cases: (i) conventional SM and (ii) integral SM control.

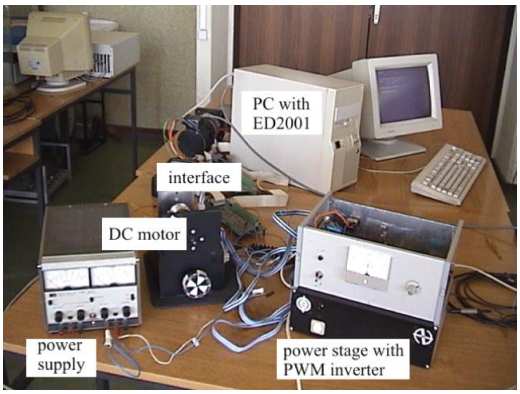

Figure 8. Experimental platform for control of DC motor.

TABLE I. CONTROLLER PARAMETERS

	Desired λ	K_{eq}	k_p	k_I
TDTSM	0	0.03975535	0.001549	0
IDTSM	-50	0.035791	0.001549	0.075546

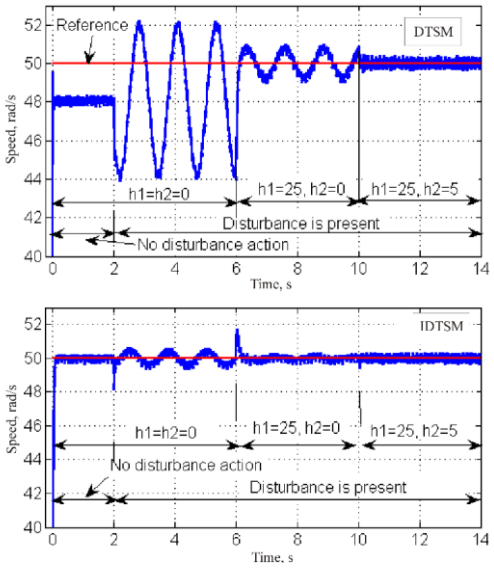

Figure 9. Experimentally obtained speed responses for different compensation configuration when disturbance $f(t)=5h(t\text{-}2)\sin(5t)$ is applied for traditionl (DTSM) and integral (IDTSM).

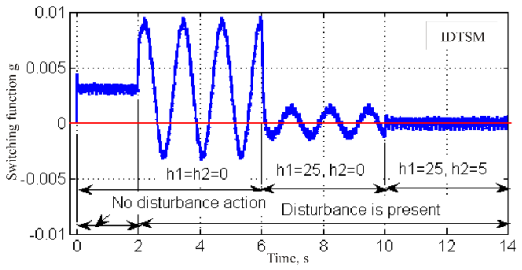

Figure 10. Experimentally obtained switching function dynamics for different compensation configurations when disturbance $f(t)=5h(t\text{-}2)\sin(5t)$ is applied in the case of IDTSM.

B. Position servo system with DC servo motor [17]

Based on (3.7), the model of the system in the error space is

$$\dot{\mathbf{e}} = \mathbf{A}\mathbf{e} + \mathbf{b}u + \mathbf{d}f;\ \mathbf{A} = \begin{bmatrix} 0 & 1 \\ 0 & -a_m \end{bmatrix};\ \mathbf{b} = \begin{bmatrix} 0 \\ -b_m \end{bmatrix};\ \mathbf{d} = \begin{bmatrix} 0 \\ 1 \end{bmatrix} \quad (7.28)$$

where: $\mathbf{e} = [e,\ \dot{e}]^{\mathrm{T}} = [e_1,\ e_2]^{\mathrm{T}}$, $e_1 = r(t) - y(t) = \theta_r - \theta_m$, $f(t) = \frac{T_L}{J} + \frac{d^2\theta_r}{dt^2} + a\frac{d\theta_r}{dt}$ is the external disturbance; T_L is the load torque, $\theta_r = r(t)$ is the referent angular position, θ_m is the angular motor shaft position, J is the overall momentum of inertia. Plant parameters are identified as: $a_m = 16,\ b_m = 680$.

The model fulfills the matching conditions [4]:

$$\operatorname{rang}[\mathbf{b} \mid \mathbf{d}] = \operatorname{rang}[\mathbf{b}]. \quad (7.29)$$

Let the control be in the form:

$$u_k = u_{s,k} - u_{I,k}, \quad (7.30a)$$

$$u_{s,k} = -\mathbf{c}_\delta \mathbf{A}_\delta \mathbf{e}_k - \min\{v_k, w_k\}\operatorname{sgn}(g_k),$$
$$v_k = |g_k|/T;\ \ w_k = \sigma + q|g_k|, \sigma = const > 0, \quad (7.30b)$$
$$q = const \geq 0;$$

$$u_{I,k} = \begin{cases} 0 & \text{if } \min\{v_k, w_k\} = w_k \text{ or } |e_{2,k}| > \rho \\ hg_k + u_{I,k-1} & \text{if } \min\{v_k, w_k\} = v_k \text{ and } |e_{2,k}| \leq \rho \end{cases} \quad (7.30c)$$

$$0 < \rho < 1,\quad 0 < h < 1/T;\ h = \alpha/T\,. \quad (7.30d)$$

A PC with an acquisition and control card realizes the digital control algorithm. A 12-bit D/A converter feed the control signal to the system. The sampling period of T=0.4 ms is used. DT model of the nominal system (6.1) is

$$\delta\begin{bmatrix} e_{1,k} \\ e_{2,k} \end{bmatrix} = \begin{bmatrix} 0 & 0.9968 \\ 0 & -15.9489 \end{bmatrix}\begin{bmatrix} e_{1,k} \\ e_{2,k} \end{bmatrix} + \begin{bmatrix} -0.13571 \\ -677.828635 \end{bmatrix} u_k\,. \quad (7.31)$$

The matching conditions (7.29) do not hold, but due to the small sampling period, degradation of the matching conditions may be neglected.

Fig. 11 gives the block-structure of the DC-motor positional servo system. Experimental platform is given in Fig. 8. Some experimental and simulation results are presented in Figs. 12 to 14. Value λ is set to -15, as in [8]. The controller parameters are $[c_{\delta 1}\ \ c_{\delta 2}] = [-0.0221\ \ -0.0015]$, $\mathbf{c}_\delta\mathbf{A}_\delta = [k_1\ \ k_2] = [0\ \ 0.0015]$. The switching gains are chosen to be $\sigma = 10$ and $q = 0$.

All simulation and experimental results verify that the used control approaches, enhanced by the additional disturbance compensation, provide excellent performances.

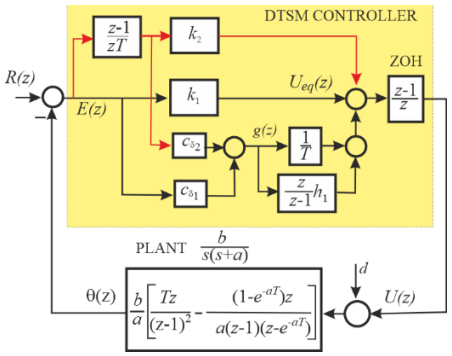

Figure 11. Structure of DC-motor position control system in linear control mode.

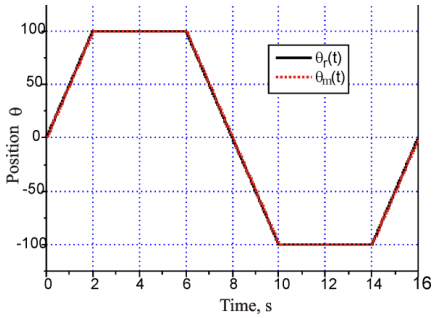

Figure 12. Referent position profile $\theta_r(t)$ and the obtained motor shaft position $\theta_m(t)$ using the proposed control.

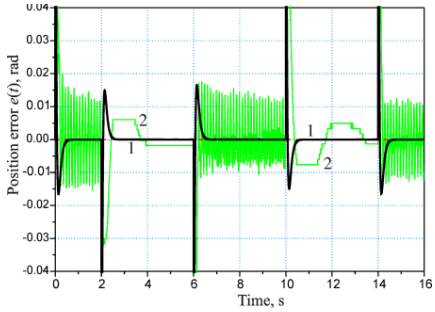

Figure 13. Tracking error of the referent position profile (Fig. 12): the proposed system (ρ=0.5, h=16): 1- simulation, 2-experiment,

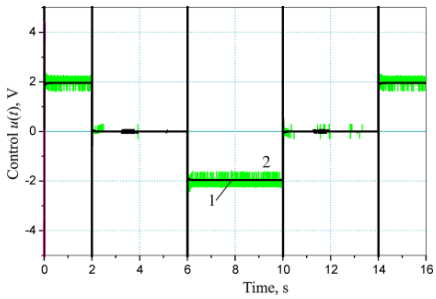

Figure 14. Control signal. 1 – simulation; 2- experiment

C. *Speed control of IM motors* [25]

By using the FOC technique, IM speed control can be effectively organized by using the method given in Subsection 7.A. Block diagram of IM speed control system is presented in Fig. 4, in which controller C_3 is not present, and PI controllers are used in inner current control loops.

IM is more complex than DC motor. It is a nonlinear and highly coupled plant. Our preliminary investigations and experiments have affirmed the possibility of using IDTSM for speed control of IM. The IDTSM speed controller for this case is given in Fig. 15. Block Int 1 is the switching function integrator in equation (6.21), whose limit is set to ±0.01. Block Int 2 denotes the integrator of the disturbance compensator (6.33).

Sampling time is 0.1 ms for FOC and 1 ms for speed control. Simulations and experiments have been conducted in accordance with Fig. 15.

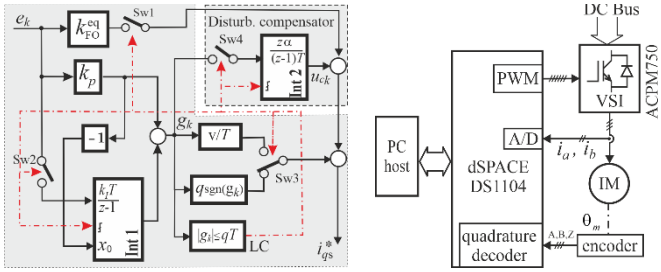

Figure 15. IDTSM controller for IM (left); Block diagram of experimental setup speed control (right).

IDTSM controller with disturbance compensator (6.33) with suitably chosen gain h_1 gives excellent results presented in Figs 17 - 21 where comparisons with conventional PI control are given. Parameters of IM motor are given in Table II, and parameters of conventional PI and the proposed IDTSM controllers are given in Tables III and IV, respectively. An experimental setup is presented in Fig. 16 and its schematic diagram in Fig. 15 (right).

TABLE II. RATED PARAMETERS OF THE IM1 [25]

Nominal power [W]	1500	Phase voltage [V]	230	Rotor resistance [Ω]	3.1852
Nominal speed [rpm]	2860	Phase current [A]	3.25	Total stator inductance [H]	0.4531
Total inertia [kgm^2]	0.0035	Frequency [Hz]	50	Magnetizing inductance [H]	0.4413
Friction coeff. [Nms/rad]	0.0022	Stator resistance [Ω]	5.45	Total rotor inductance [H]	0.4531

TABLE III. PARAMETERS OF THE CONVENTIONAL PI TYPE CONTROLLERS

Current controllers	K_p=22.3977	K_i=0.87466
Speed controller	$K_{p\omega}$=0.4443	$K_{i\omega}$=0.0198

TABLE IV. PARAMETERS OF THE PROPOSED SM SPEED CONTROLLER

λ=-50	k_p= 0.0024978	k_I=0.1218199
k_{FO}^{eq} = 0.12105	k_{RO}^{eq} = 7.695e-04	q=8, h=50

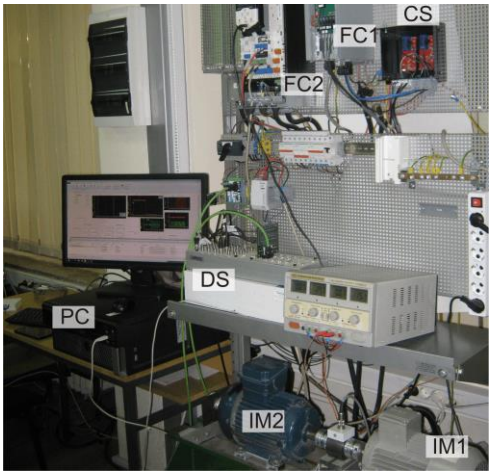

Figure 16. Experimental setup: PC – personal computer with Control Desk DS - DS1103 dSPACE controller, FC1 and IM1 – frequency converter and IM under test, FC2 and IM2 – frequency converter and IM for load torque generation, CS – current sensors

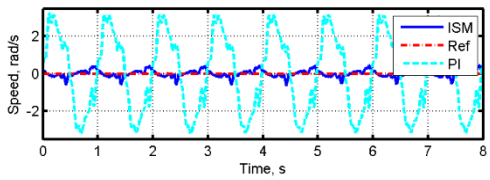

Figure 17. Speed response for zero reference with load $T_L(t) = 5\sin(2\pi t)$

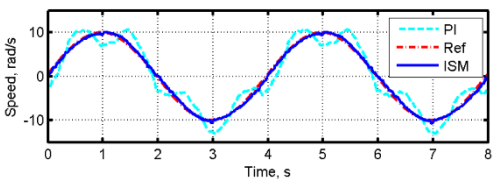

Figure 18. Tracking of reference $\omega^*(t) = 10\sin(\pi t)$ with load $T_L(t) = 5\sin(2\pi t)$.

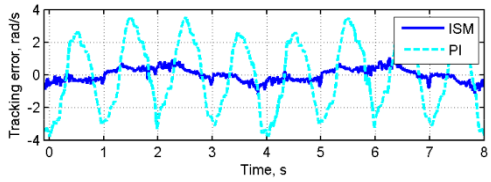

Figure 19. Tracking errors from Fig. 18.

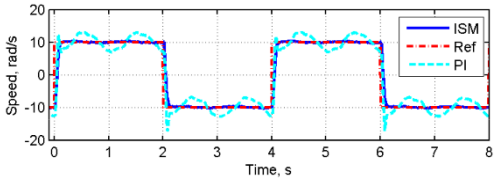

Figure 20. Tracking of pulse train ±10 rad/s with load $T_L(t) = 5\sin(2\pi t)$.

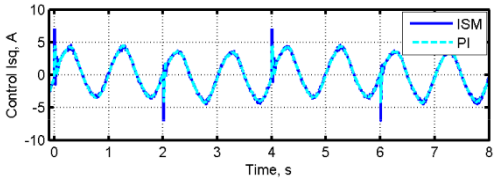

Figure 21. *q*- axis current reference, as output (control signal) of the speed controller for Fig. 20 case

D. Cascade Control of IM [24]

Design and experimental results are obtained according to structure in Fig. 6, on the experimental platform, Fig. 15, with the nominal parameters of IM given in Table II. FOC subsystem, including current controllers, has sample-time 0.1 ms. The speed controller is discretized by sample time of 0.5 ms and position controller with 1 ms. All controllers are fully DTSM-based according to equations (6.36) excluding (6.36j), which is used only in the position controller.

Table V gives parameters of the controlled plants and the corresponding controllers.

TABLE V. PARAMETERS OF CONTROLLERS [24]

***q*-axis current controller**
$a_i = -233.8936$, $b_i = 42.8992$, $k_{eq} = -5.4521$,$c_\delta = 0.0236$, $k_{r1} = 0.25$, $k_{r2} = 0.3$, $k_{int} = 1000$, $U_0 = \sqrt{2}\cdot 230$, $\beta = 0.001$
Speed controller
$a_\omega = -0.6286$, $b_\omega = 340.7439$ $k_{eq.} = -0.0015$, $c_\delta = 0.0025$, $k_{r1} = 0.12$, $k_{r2} = 0.8$ $k_{int} = 100$, $U_0 = 5.02$, $\beta = 0.5$
Position controller
$\mathbf{A} = [0, 1; 0, -500]$, $\mathbf{b} = [0;500]$ $\mathbf{k}_{eq} = [0, -0.9373]$, $\mathbf{c}_\delta = [0.0627, 0.0025]$, $k_{r1} = 0.9$, $k_{r2} = 0.1$, $k_{int} = 40$, $U_0 = 30$, $\alpha = 1$, $\beta = 0.001$

The experimentally obtained results (with mechanical load profile $T_L = 5\cdot\left[h(t-2) - h(t-4) + h(t-8)\cdot\sin(4\pi t)\right]$ are given in Figs. 22 to 27, which indicate high-performance of the proposed design of EDs control systems via DTSM

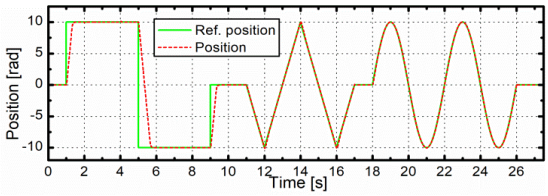

Figure 22. Position tracking

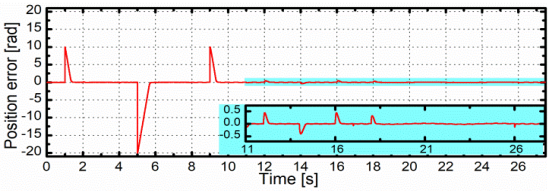

Figure 23. Position tracking error

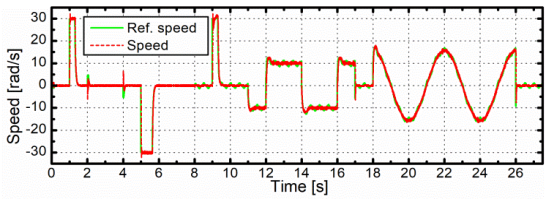

Figure 24. Speed reference (output of the position controller, solid line) and the estimated motor speed (dashed line)

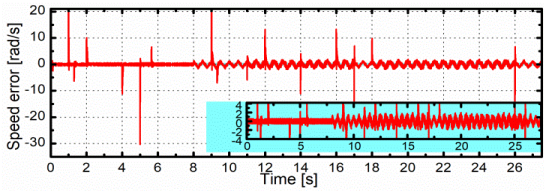

Figure 25. Speed error (speed sliding variable)

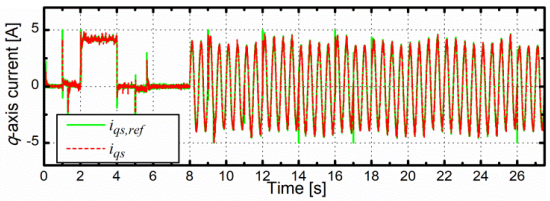

Figure 26. Torque producing current component: reference current (output of the speed controller – solid line), the actual current i_{qs} (dashed line)

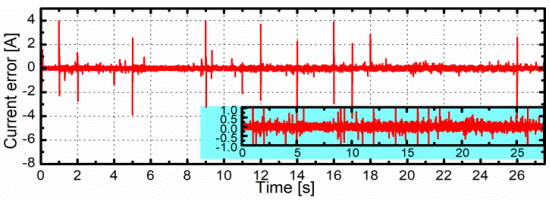

Figure 27. Current error (current sliding variable)

VIII. CONCLUSIONS

This paper is an overview of our investigations in the area of EDs control by using DTSM. In order to give a complete view

to modern approaches in EDs control, an appropriate attention is paid to the generalized mathematical model of two-phase machine and the corresponding coordinate transformations, which lay the modern basis of IM and PMSM control.

To simplify the position (speed) controller design, mathematical models of DC motor and IM have been approximated by a second (first) order dynamics, thus making the controller design simpler.

DT controller synthesis is made by using original design methods, known as robust DT chattering free SM control and a comprehensive method for determining parameters of the switching function.

Furthermore, two methods for improving robustness are underlined in this paper. The first method uses the integral action of the switching function to improve disturbance rejection property and reference tracking accuracy. The second method uses the super-twisting-like control principle as an effective approach to disturbance rejection.

Practically realized servo systems are briefly illustrated by the experimentally obtained results, offering the references to the used control structures. More details of the presented investigations can be found in the given references

REFERENCES

[1] F. Blaschke, “The principle of field orientation as applied to the newtransvector closed-loop control system for rotating field machines,” Siemens Review, vol. 34, no. 5, pp. 217-220, 1972.

[2] М. Г. Чиликин, В. И. Ключев, А.С. Сандлер, Теория автоматизированного электропривода, 'Энергия', 1979.

[3] B. Veselić, B. Peruničić-Draženović, Č. Milosavljević, “High-Performance Position Control of Induction Motor Using Discrete-Time Sliding Mode Control,” IEEE Trans. on Ind. Electron., vol. 55, no. 11, pp. 3809-3817, 2008.

[4] B. Draženović, “The Invariance Conditions in Variable Structure Systems,“ Automatica, vol. 5, no. 3, pp. 287-295, 1969.

[5] X. Yu, B. Wang, X. Li, “Computer-Controlled Variable Structure Systems: The State of Arts,” IEEE Trans. on Ind. Informatics, vol. 8, no. 2, pp. 197-205, May 2012.

[6] R. H. Midleton, G. C. Goodwin, “Improved Finite Word Length Characteristics in Digital Control Using Delta Operators,” IEEE Trans. on Automatic Control, vol. 31, no. 11, pp. 1015-1021, 1986.

[7] W. C. Su, S. V. Drakunov, Ü. Özguner, “Implementation of Variable Structure Control for Sampled Data Systems,” in: Garofalo, F., Glielmo, L. E. (Eds.): Robust Control via Variable Structure and Lyapunov Techniques, Springer Verlag, London, 1996, pp. 87-106

[8] G. Golo, Č. Milosavljević, "Robust Discrete-Time Chattering-free Sliding Mode Control Systems,” System and Control Letters, vol. 41, no. 1, pp. 19-28, 2000.

[9] X. Shao, D. Sun, “Development of a New Robot Controller Architecture with FPGA-Based IC Design for Improved High-Speed Performance,” IEEE Trans. on Ind. Informatics, vol. 3, no. 4, pp. 312-321, Nov. 2007.

[10] Z. Bučevac, Design of Digital Discrete Control Systems With Sliding Mode, Ph. D. Dissertation, University of Belgrade, Faculty of Mechanical Engineering, 1985 (in Serbo-Croatian).

[11] A. Salihbegović, Contribution to Analysis and Synthesis of Discrete Realized Systems With Switched Control, Ph.D. Dissertation, University of Sarajevo, Faculty of Electrical Engineering, Sarajevo, 1985 (in Serbo-Croatian)

[12] S. V. Drakunov, V. I. Utkin, “On Discrete-Time Sliding Mode,” Proc. IFAC Symposium on Nonlinear Control Systems Design, Capry (Italy, 1989) pp. 484-489

[13] K. Abidi, J.-X. Xu, X. Yu, "On the discrete-time integral sliding modecontrol," IEEE Trans. on Automatic Control, vol. 52, no. 4, pp. 709-715, Apr. 2007.

[14] Č. Milosavljević, B. Peruničić-Draženović, B. Veselić, “Discrete-Time Velocity Servo System Design Using Sliding Mode Control Approach with Disturbance Compensation,” IEEE Trans on Ind. Informatics, vol. 9, no. 2, pp. 920-927, May, 2013.

[15] B. Draženović, Č. Milosavljević, B. Veselić, “Comprehensive Approach to Sliding mode Design and analysis Linear Systems,” in: Advances in Sliding Mode Control, Concept, Theory and Implementation, pp. 1-19, Springer, Berlin Heidelberg, 2013

[16] G. Bartolini, A. Ferrara, V. I. Utkin, “Adaptive sliding mode control in discrete-time systems,” Automatica, vol. 31, no. 5, pp. 769–773, 1995.

[17] Č. Milosavljević, B. Draženović, B. Veselić, D. Mitić, “A New Design of Servomechanisms with Digital Sliding Mode,” Electrical Engineering, vol. 89, no. 3, pp. 233-244, 2007.

[18] C. Y.Chan, “Robust Discrete-Time Sliding Mode Controller,” Systems & Control Letters, vol. 23, no. 5, pp. 371-374, 1994.

[19] M. Lješnjanin, B. Peruničić, Č. Milosavljević, B. Veselić,"Disturbance compensation in digital sliding mode", In: 2011 IEEE EUROCON-International Conference on Computer as a Tool, (Lisboa, Portugal 2011), pp. 1-4.

[20] V. I. Utkin, “Sliding mode control design principles and applications to electric drives,” IEEE Trans. Ind. Electron., vol. 40, no. 1, pp. 23-36, Feb. 1993.

[21] M. B. Naumović, “Some approaches to velocity estimation in digital controlled DC servo drives,” in Proc. 6th Int. Conf. Systems, Automatic Control and Measurements, Niš, Yugoslavia, 1998, pp. 140-144

[22] A. Chalanga, S. Kamal, L. Fridman, B. Bandyopadhyay, J. A. Moreno, “How to implement Super-Twisting Controller based on sliding mode observer?,” In 2014 13th International Workshop on Variable Structure Systems (VSS), pp. 1-6.

[23] B. Veselić, B. Peruničić-Draženović, Č. Milosavljević, “Improved discrete-time sliding-mode position control using Euler velocity estimation,” IEEE Trans. Ind. Electron., vol. 57, no. 11, pp. 3840–3847, 2010.

[24] M. Petronijević , Č. Milosavljević, B Veselić, B. Peruničić-Draženović, S. Huseinbegović, “Robust cascade control of electrical drives using discrete-time chattering free sliding mode controllers with output saturation,” Electrical Engineering, pp.1-15, 2021.

[25] Č. Milosavljević, B. Peruničić-Draženović, B. Veselić, M. Petronijević, “High-performance discrete-time chattering-free sliding mode based control of induction motor,” Electrical Engineering, vol. 99, no. 2, pp. 583–593, 2017.